

PAPER • OPEN ACCESS

Effects of direct interactions on deuteron induced reactions¹

To cite this article: M. Avrigeanu and V. Avrigeanu 2018 *J. Phys.: Conf. Ser.* **1023** 012009

View the [article online](#) for updates and enhancements.

You may also like

- [On deuteron interactions within surrogate reactions and nuclear level density studies](#)
M. Avrigeanu and V. Avrigeanu
- [Consistent analysis of deuteron interactions at low and medium energies](#)
M. Avrigeanu and V. Avrigeanu
- [On the overlap of the pre-equilibrium and direct reaction models](#)
M Avrigeanu, D Bucurescu, M Ivascu et al.



ECS
The
Electrochemical
Society
Advancing solid state &
electrochemical science & technology

DISCOVER
how sustainability
intersects with
electrochemistry & solid
state science research

Effects of direct interactions on deuteron induced reactions¹

M. Avrigeanu and V. Avrigeanu

Horia Hulubei National Institute for Physics and Nuclear Engineering, P.O. Box MG-6, 76900 Bucharest, Romania

E-mail: marilena.avrigeanu@nipne.ro

Abstract. A detailed analysis of the direct-interaction key role in the deuteron-induced reactions on target nuclei from Al to U has been carried out. Particular comments concern the main importance of the deuteron breakup mechanism in the deuteron interaction with heavy target nuclei at incident energies around Coulomb barrier.

1. Introduction

An update of the theoretical analysis of deuteron-nuclei interaction within an unitary and consistent account of the related reaction mechanisms is highly requested by on-going strategic research programs as the International Thermonuclear Experimental Reactor (ITER) [1], the International Fusion Material Irradiation Facility (IFMIF) [2], in connection with the ITER program, and the Neutron For Science (NFS) project at SPIRAL-2 facility [3]. The discrepancies between the existing deuteron experimental data and even the latest version of the evaluated data library TENDL-2015 [4] demand further measurements as well as improved model calculations so that the deuteron evaluated data libraries may approach the standard of the current neutron data libraries.

So far the Hauser-Feshbach statistical model has been involved as the main tool to calculate the deuteron reaction cross sections at low and medium incident energies, the compound-nucleus (CN) mechanism being considered to be dominant within this energy range. However, specific non-compound processes make the reactions induced by deuterons different from those induced by other incident particles [5, 6, 7, 8]. The deuteron interaction at incident energies below and around the Coulomb barrier proceeds largely through direct reaction (DR) mechanisms of stripping and pick-up, while the pre-equilibrium emission (PE) and evaporation from CN become important with the increase of the incident energy. Moreover, in addition to these well known reaction mechanisms, the specific deuteron breakup (BU) process plays an important role that increases the complexity of the deuteron interaction analysis in the whole incident energy range due to the large variety of reactions initiated by the BU nucleons at their turn.

2. Deuteron breakup

While the theoretical models for DR, PE, and CN are already settled, an increased attention should be paid to the description of the BU mechanism and its components, namely the

¹ International School on Nuclear Physics and Applications, September 10-16, 2017 Varna, Bulgaria



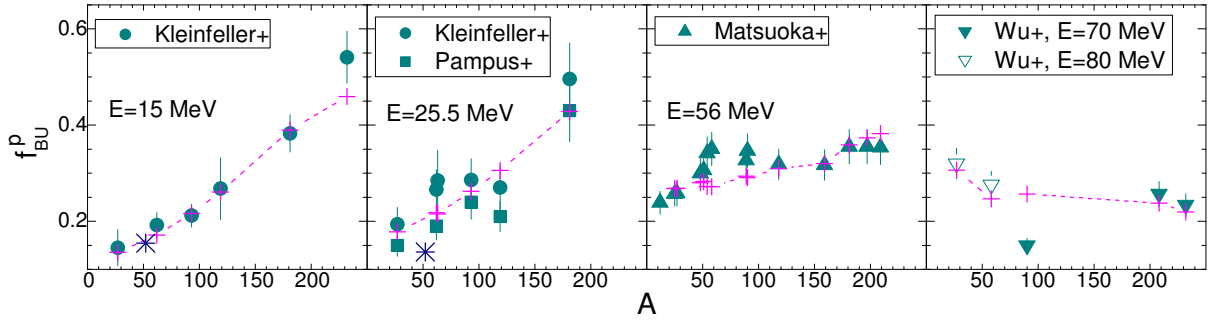


Figure 1. Comparison of the measured [13, 14, 15, 16] total BU proton-emission fractions with the empirical parametrization predictions (crosses) [11], connected by dashed lines for eye guiding, for target nuclei from ^{12}C up to ^{232}Th , at the deuteron energies of 15, 25.5, 56, 70, and 80 MeV.

elastic breakup (EB), in which the target nucleus stays in its ground state and both deuteron constituents fly apart, and the inelastic breakup or breakup fusion (BF), where one of breakup nucleons interacts non-elastically with the target nucleus. The compound nuclei in reactions induced by the BF nucleons differ by one unit of the atomic mass and maybe also atomic number than in deuteron-induced reactions, the partition of the BF cross section among various residual-nuclei population being triggered by the energy spectra of the breakup nucleons and the excitation functions of the reactions induced by these nucleons on the target nuclei [5, 6, 7, 8]. Overall, there are actually two opposite effects of the deuteron breakup on the deuteron activation cross sections that should be considered. Firstly, the deuteron total-reaction cross section σ_R , that is shared among different outgoing channels, is reduced by the value of the total BU cross section σ_{BU} . On the other hand, BU nucleons interactions with the target nucleus enhance the various reaction channels of the original deuteron interactions.

An empirical parametrization [11] of both the total breakup (EB+BF) and EB data has involved the assumption that the BF neutron-emission cross section σ_{BF}^n is the same as that for the BF proton-emission σ_{BF}^p (e.g., Ref. [12]), so that σ_{BU} is given by the sum $\sigma_{EB} + 2\sigma_{BF}^{n/p}$. This parametrization has concerned the total breakup nucleon and EB fractions, i.e. $f_{BU}^{n/p} = \sigma_{BU}^{n/p} / \sigma_R$ and $f_{EB} = \sigma_{EB} / \sigma_R$, respectively. The dependence of these fractions on the deuteron incident energy E and the target-nucleus atomic Z and mass A numbers was obtained [11] through analysis of the experimental systematics of deuteron-induced reactions on target nuclei from ^{27}Al to ^{232}Th and incident energies up to 80 MeV for the former [13, 14, 15, 16] but within a more restricted up to 30 MeV [16] energy range for the later. In the absence of available experimental deuteron EB data at incident energies above 30 MeV, the correctness of the corresponding parametrization extrapolation has been checked by comparison of the related predictions [17] with results of the microscopic CDCC method [18].

The comparison of the measured total BU proton-emission fractions σ_{BU}^p at 15 [16], 25.5 [13, 16], 56 [15], and 70 and 80 MeV [14] with the parametrization prediction for deuterons incident on target nuclei from ^{12}C to ^{232}Th is shown in Fig. 1. The same scale is used for the f_{BU}^p values at all incident energies of the available experimental data, in order to make possible also an assessment of their energy dependence. At once with the variation with energy and the mass of the target nucleus, the f_{BU}^p values illustrate the importance of the BU process among the other reaction mechanisms related to the deuteron interaction. Among other features [11] this comparison shows the BU importance increasing with the target-nucleus mass, from ^{27}Al up to ^{232}Th , at the lower incident energies of 15-25.5 MeV. This increase is less significant at the energy of 56 MeV, and even reversed at 70-80 MeV.

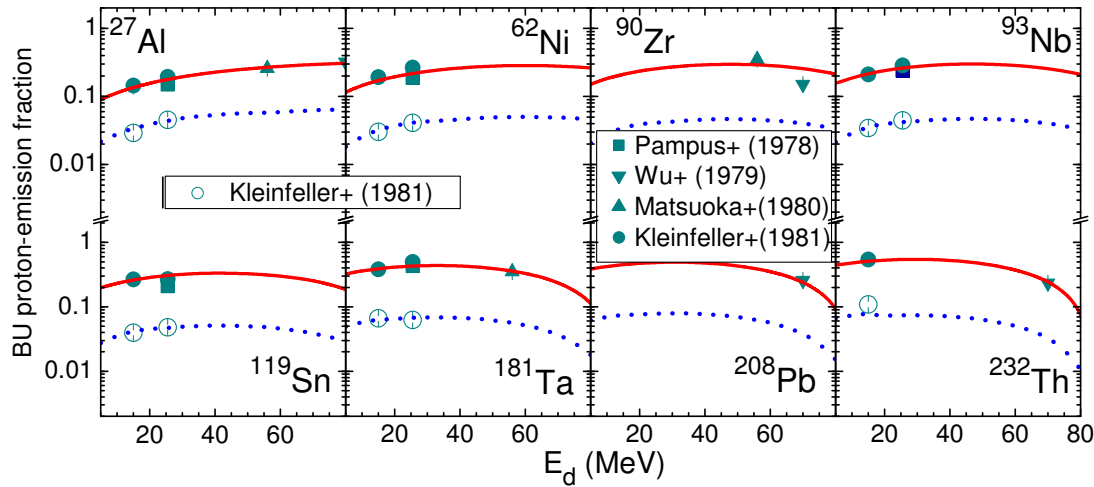


Figure 2. Comparison of experimental [13, 14, 15, 16] f_{BU}^p (solid symbols) and f_{EB} values (open circles) for deuterons incident on nuclei from Al to Th at energies up to 80 MeV. The parametrization predictions [11] are drawn by solid (f_{BU}^p) and dotted (f_{EB}) curves.

Next, the comparison between total breakup proton-emission and elastic-breakup fractions for target nuclei from ^{27}Al to ^{232}Th shown in Fig. 2 emphasizes their large difference, pointing out the dominance of the BF component ($f_{BF}^p = f_{BU}^p - f_{EB}$) over the much weaker EB component.

In order to calculate the BF enhancement of the (d, xn) reaction cross sections, the BF proton-emission cross section σ_{BF}^p should be (i) multiplied by the ratios $\sigma_{(p,x)}/\sigma_R^p$, corresponding to the enhancing reaction, (ii) convoluted with the Gaussian line shape of the BF-proton energy E_p for a given deuteron incident energy E_d , and followed by (iii) an integration over the BF proton energy. Consequently, the BF-enhancement cross section has the form [5, 6, 7]:

$$\sigma_{BF}^{p,x}(E_d) = \sigma_{BF}^p(E_d) \int_0^{E_d - B_d} dE_p \frac{\sigma_{(p,x)}(E_p)}{\sigma_R^p} \frac{1}{(2\pi)^{\frac{1}{2}} w} \exp\left[-\frac{(E_p - E_p^0)^2}{2w^2}\right], \quad (1)$$

where B_d is the deuteron binding energy, σ_R^p is the proton total reaction cross section, x stands for various γ , n , d , or α outgoing channels, while the Gaussian distribution parameters w and E_p^0 are given by Kalbach [19].

To reduce as much as possible the supplementary uncertainties brought by additional theoretical calculations, the $\sigma_{(p,x)}$ values are taken from the experimental EXFOR library [20], while σ_R^p is provided by a proton optical model potential [21].

The BF enhancement could be quite important as it was shown [7] for the study of $^{231}\text{Pa}(d,3n)^{230}\text{U}$ reaction around the Coulomb barrier. In this case the absorbed BF proton contributes to enhancement of the ^{230}U activation cross section through $^{231}\text{Pa}(p,2n)^{230}\text{U}$ reaction. In order to calculate the corresponding BU enhancement, the convolution of the ratio of $(p,2n)$ reaction cross section [20] and proton total-reaction cross section - that corresponds to the weight of the $(p,2n)$ reaction induced by the BF protons on ^{231}Pa target nuclei - with the Gaussian distribution of the BU-proton energies corresponding to a given incident deuteron energy [19] was carried out as shown in Fig. 3(a) for three deuteron energies. The area of the related convolution results corresponds to the BF enhancement of $(d,3n)$ reaction cross sections at each deuteron energy. The energy dependence of this BF enhancement to $^{231}\text{Pa}(d,3n)^{230}\text{U}$ activation cross section is shown in Fig. 3(b), where the corresponding total calculated activation of ^{230}U is finally compared with experimental data. As expected, the realistic treatment of the BF enhancement

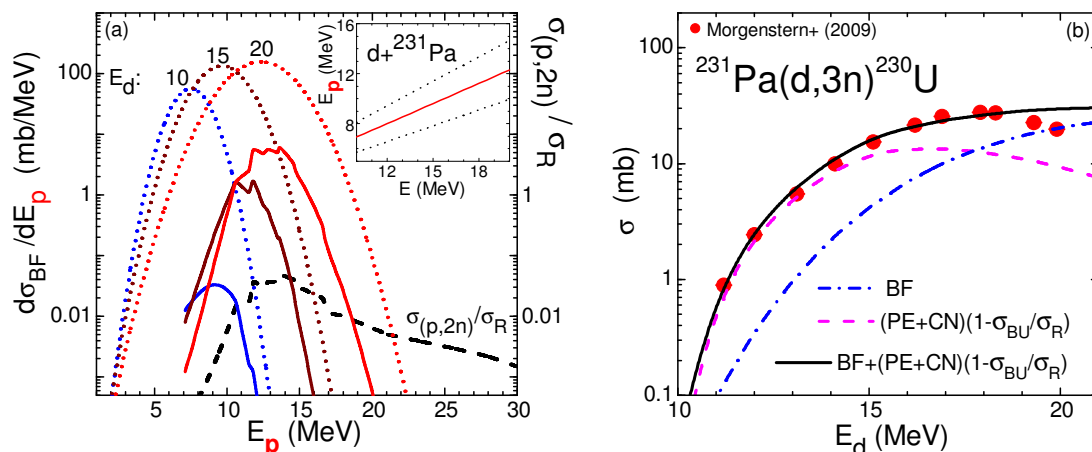


Figure 3. (a) BF enhancement (solid curves) to the $^{231}\text{Pa}(d,3n)^{230}\text{U}$ reaction obtained from the convolution of the cross sections ratio $\sigma_{(p,2n)}/\sigma_R^p$ for the target nucleus ^{231}Pa (dashed curve) with the Gaussian distribution (dotted curves) of breakup-proton energies for deuterons on ^{231}Pa at incident energies of 10, 15 and 20 MeV as noted on their top; (b) BF enhancement (dash-dotted curve) to the $^{231}\text{Pa}(d,3n)^{230}\text{U}$ reaction excitation function (solid curve) [7] in addition to PE+CN contribution corrected for initial flux leakage towards BU (dashed curve) (see text).

by taking into account the large widths of BU-proton energy distributions shown in the upper insertion of Fig. 3(a) led to a rather accurate description of data.

3. Transfer reactions

Apart from the BU contributions to deuteron interaction, an increased attention has to be devoted to the DR, in spite of related very poor attention or being even not accounted so far in deuteron activation analysis. The calculation of the DR stripping (d, p) and (d, n), and pick-up (d, t) and (d, α) mechanism contributions has been performed using the distorted-wave Born approximation (DWBA) method within the FRESKO [22] computer code. The post/prior form distorted-wave transition amplitudes for ($d, n/p$) stripping and respectively ($d, t/\alpha$) pick-up reactions, and the finite-range interaction have been considered in this respect. The n - p effective interaction in deuteron [23] as well as d - n effective interaction in triton [24] were assumed to have a Gaussian shape, at the same time with a Woods-Saxon shape [25] of the d - d effective interaction in the α particle. The transferred nucleon and deuteron bound states were generated in a Woods-Saxon real potential [5, 6, 8] while the transfer of the deuteron cluster has been taken into account for the (d, α) pick-up cross section calculation. The populated discrete levels and the corresponding spectroscopic factors which have been available within the ENSDF library [26] were used for the DWBA calculations.

The suitable description of the experimental proton, neutron, triton, and alpha-particle angular distributions, for stripping and pick-up transitions, respectively, to states of the corresponding residual nuclei, has been standing for the validation of the spectroscopic information used and the finally calculated total stripping and pick-up reaction cross sections [5, 6, 9, 10]. Thus, the description of the experimental double-differential cross sections of the populations of low-lying levels in ^{239}U and ^{237}U through $^{238}\text{U}(d,p)^{239}\text{U}$ and $^{238}\text{U}(d,t)^{237}\text{U}$ stripping and pick-up reactions, respectively, shown in in Fig. 4(a,b), validates the correctness of the DR cross-section calculations. Consequently it has been proved the accuracy of the corresponding (d,p) and (d,t) total excitation functions in Fig. 4(c, bottom). Sum of the total (d,p), (d,t), and BU cross sections gives a lower limit of the DI contribution to the deuteron

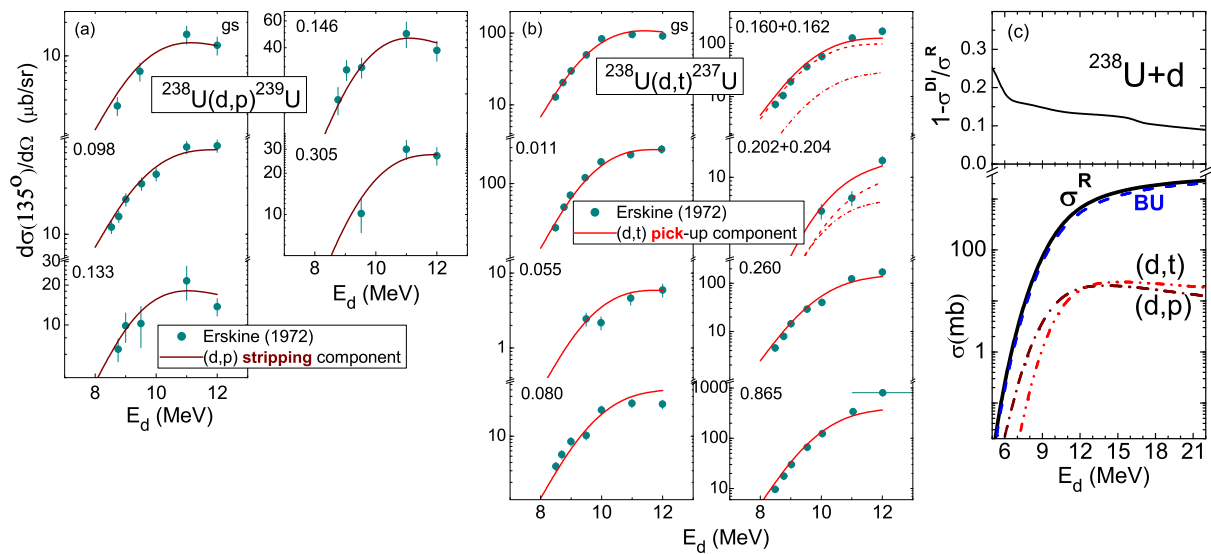


Figure 4. Comparison of calculated (solid curves) and measured [27] excitation functions for the populations at 135° of low-lying levels in (a) ^{239}U and (b) ^{237}U , through (d,p) and (d,t) direct reactions, respectively. (c) (bottom) BU (dashed curve), stripping (dash-dotted curve), and pick-up (dash-dot-dotted curve) cross sections for deuterons on ^{238}U , and the reduction factor of the deuteron flux going towards statistical processes (top) [9].

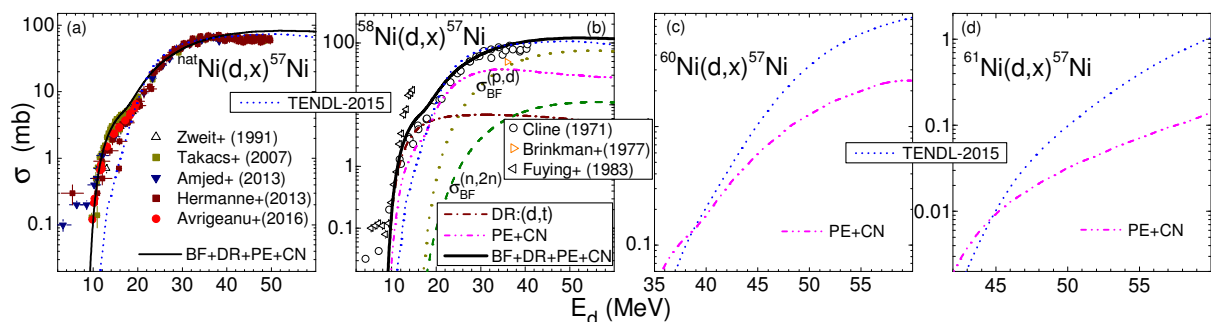


Figure 5. Comparison of measured [6, 20], TENDL-2015 [4] evaluated (short-dotted curves), and theoretically predicted (solid curves) cross sections for $^{nat}\text{Ni}(d,x)^{57}\text{Ni}$ reactions, with due consideration of contributions from the BF enhancement (dashed and dotted curves), pick-up DR (dash-dotted curve), and PE+CN (dash-dot-dotted curves) reaction mechanisms [6].

interaction with ^{238}U target nucleus, while the deuteron total-reaction cross section that remains to be available for the PE+CN mechanisms has to be corrected for the incident-flux leakage through the DI processes [5, 6, 9, 10] shown on top of Fig. 4(c). Results presented in Fig. 4(c) point out the DI (mainly breakup) dominant role in the deuteron interaction with ^{238}U around Coulomb barrier, which is a specific feature for the heavy target nuclei [13, 16].

The lack of due consideration of the DI mechanisms within theoretical frame of deuteron surrogate-reaction method should be considered the main reason for the failure of the $(d,p\gamma)$ surrogate-reaction validation tests comparing already well-known (n,γ) cross sections with those provided by deuteron surrogate reaction $(d,p\gamma)$ [28]. Our detailed analyzes [9, 10] of the nuclear reaction mechanisms involved in the $(d,p\gamma)$ surrogate reactions on ^{232}Th and ^{238}U target nuclei have pointed out the key role of the direct interactions, i.e. breakup, stripping and pick-up

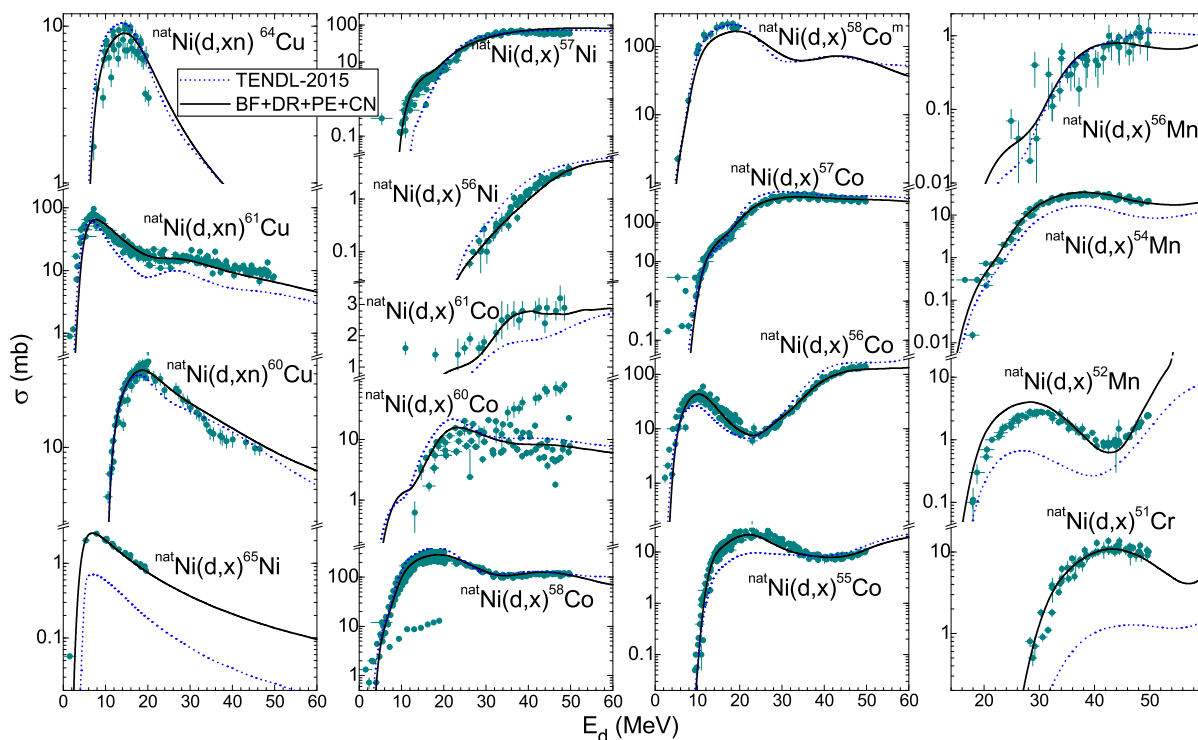


Figure 6. Comparison of measurements (solid circles) [6, 20], TENDL-2015 [4] evaluation (short-dotted curves), and model calculations (solid curves) of excitation functions for deuteron-induced reactions on ^{nat}Ni [6].

mechanisms, while only the CN mechanism was considered by the above-mentioned studies ([28] and Refs. therein).

A particular note of transfer reactions signature should concern the (d,t) pick-up reaction. In spite of being usually neglected in deuteron activation analysis, the (d,t) pick-up process is fully responsible for the lowest-energy side of the corresponding (d,x) excitation function, e.g., Fig. 5(a,b), namely at the energies between its threshold and those of the (d,dn) and (d,p2n) reactions that contribute to the population of the same residual nucleus [5, 6].

4. Statistical particle emission

The statistical PE+CN reaction mechanisms which complete the deuteron interaction analysis along an enlarged nuclear-interaction time scale, become important with the increase of the incident energy above the Coulomb barrier. The corresponding reaction cross sections are calculated using the TALYS [21] code, taking into account also the above-discussed BU, stripping, and pick-up results through a reduction factor of the OMP total-reaction cross section, given by the sum of the DI cross-sections. Another particular point of these calculations is the use of the same model parameters to account for different reaction mechanisms as, e.g., the same OMP parameters for calculation of transmission coefficients as well as PE transition rates (using the value 3 for the preeqmode TALYS keyword). Additional PE+CN calculations have been carried out with the code STAPRE-H [29] if other particular options of various input parameters could be useful (e.g., for gamma-ray strength functions or initial p-h configurations). The due consideration of all BU+DR+PE+CN is proved by the description of all measured data corresponding to deuteron interaction with a specific natural element target [5, 6], e.g., activation excitation functions for $d+^{nat}\text{Ni}$ interaction process shown in Fig. 6 [6].

5. Conclusions

The present work has concerned a deeper analysis of the key role of DI, particularly of the breakup mechanism, in deuteron-induced reactions. The overall agreement between the measured data and model calculations supports the description of nuclear mechanisms taken into account for the deuteron-nucleus interaction, emphasizing the effects of direct interactions so far ignored in the evaluation procedures.

However, while the associated theoretical frames are already settled for stripping, pick-up, PE and CN mechanisms, an increased attention should be given to the breakup mechanism. Thus further work has to be done concerning its theoretical description including the inelastic component. The improvement of deuteron breakup description requires complementary experimental studies involving deuterons, protons and neutron induced reactions too.

Acknowledgments

This work has been partly supported by Autoritatea Nationala pentru Cercetare Stiintifica (PN-16420102) and partly carried out within the framework of the EUROfusion Consortium and has received funding from the Euratom research and training programme 2014-2018 under grant agreement No 633053. The views and opinions expressed herein do not necessarily reflect those of the European Commission.

References

- [1] <http://www.iter.org/proj>
- [2] <http://www.ifmif.org/b/>
- [3] <http://pro.ganil-spiral2.eu/spiral2/instrumentation/nfs>
- [4] A.J. Koning *et al.* Dec. 2015, *TENDL-2015*, <http://www.talys.eu/TENDL2015/>
- [5] P. Bém *et al.* 2009 *Phys. Rev. C* **79**, 044610; E. Šimečková *et al.* 2011 *Phys. Rev. C* **84**, 014605; M. Avrigeanu *et al.* 2013 *Phys. Rev. C* **88**, 014612; M. Avrigeanu *et al.* 2014 *Phys. Rev. C* **89**, 044613;
- [6] M. Avrigeanu *et al.* 2016 *Phys. Rev. C* **94**, 014606
- [7] M. Avrigeanu, V. Avrigeanu, and A.J. Koning 2012 *Phys. Rev. C* **85**, 034603
- [8] M. Avrigeanu and V. Avrigeanu 2015 *Phys. Rev. C* **92**, 021601
- [9] M. Avrigeanu, V. Avrigeanu, and C. Costache 2017 *EPJ Web of Conferences* **146** 12020; M. Avrigeanu, V. Avrigeanu, and C. Costache 2017 arXiv:1703.05956v1 [nucl-th], 17 March.
- [10] M. Avrigeanu and V. Avrigeanu 2016 *J. Phys: Conf. Ser.* **724**, 012003; 2015 CERN-Proceedings-2015-001, 203
- [11] M. Avrigeanu *et al.* 2009 *Fusion Eng. Design* **84**, 418; M. Avrigeanu and V. Avrigeanu 2017 *Phys. Rev. C* **95**, 024607
- [12] M.G. Mustafa, T. Tamura, and T. Udagawa 1987 *Phys. Rev. C* **35**, 2077
- [13] J. Pampus *et al.* 1978 *Nucl. Phys. A* **311**, 141
- [14] J.R. Wu, C.C. Chang, and H.D. Holmgren 1979 *Phys. Rev. C* **19**, 370
- [15] N. Matsuoka *et al.* 1980 *Nucl. Phys. A* **345**, 1
- [16] J. Kleinfeller *et al.* 1981 *Nucl. Phys. A* **370**, 205
- [17] M. Avrigeanu and A. M. Moro 2010 *Phys. Rev. C* **82**, 037601
- [18] M. Kamimura *et al.* 1986 *Prog. Theor. Phys.* **89**, Suppl. 1, 1; N. Austern *et al.* 1987 *Phys. Rep.* **154**, 125; A. Deltuva *et al.* 2007 *Phys. Rev. C* **76**, 064602; K. Ogata and K. Yoshida 2016 *Phys. Rev. C* **94**, 051603(R)
- [19] C. Kalbach Walker 2003 *TUNL Progress Report XLII (2002-2003)*, p. 82-83
- [20] Experimental Nuclear Reaction Data (EXFOR), www-nds.iaea.org/exfor
- [21] A.J. Koning, S. Hilaire, and S. Goriely 2015 v. TALYS-1.8, <http://www.talys.eu>
- [22] I.J. Thompson 1988 *Comput. Phys. Rep.* **7**, 167; 2011 v. FRES 2.9
- [23] M. Kawai, M. Kamimura, and K. Takesako 1969 *Prog. Theor. Phys. Suppl.* **184**, 118
- [24] P. Guazzoni *et al.* 2011 *Phys. Rev. C* **83**, 044614
- [25] R.M. DelVecchio 1973 *Phys. Rev. C* **7**, 677
- [26] Evaluated Nuclear Structure Data File (ENSDF), <http://www.nndc.bnl.gov/ensdf/>
- [27] J.R. Erskine 1972 *Phys. Rev. C* **5**, 959
- [28] J.N. Wilson *et al.*, 2012 *Phys. Rev. C* **85**, 034607; Q. Ducasse *et al.* 2016 *Phys. Rev. C* **94**, 024614
- [29] M. Avrigeanu and V. Avrigeanu 1995 *IPNE Report NP-86-1995*, Bucharest, and Refs. therein; <http://www.oecdnea.org/tools/abstract/detail/iaea0971/>